Enhancement of electron correlations and spin density wave fluctuations of the organic superconductor λ-$(BETS)_2GaCl_4$ under pressure proved by ^{13}C NMR

M. Sawada* and A. Kawamoto†
Department of Condensed Matter Physics, Graduate School of Science, Hokkaido University, Sapporo 060-0810, Japan

T. Kobayashi
Graduate School of Science and Engineering, Saitama University, Saitama 338-8570, Japan

(Received 29 October 2020; revised 23 December 2020; accepted 23 December 2020; published 11 January 2021)

We performed ^{13}C NMR measurements on an organic superconductor λ-$(BETS)_2GaCl_4$ [BETS: bis(ethylenedithio)tetraselenafulvalene] to investigate the pressure effect on the spin density wave (SDW) fluctuations at low temperatures, which were observed at ambient pressure. We found that the spin-lattice relaxation rate divided by temperature $(1/T_1T)$ is significantly enhanced at low temperatures at 3 kbar, implying enhancement of the SDW fluctuation. When further pressure is applied, increase in $1/T_1T$ at low temperatures is suppressed and $1/T_1T$ becomes temperature independent, indicating the Fermi liquid state. Moreover, we revealed that the Korringa factor under pressure becomes double compared to its value at ambient pressure, suggesting a significant change in electron correlation. We discuss the effect of the SDW fluctuation and the electron correlation on the unconventional superconductivity.

DOI: 10.1103/PhysRevB.103.045112

I. INTRODUCTION

Research on organic conductors has significantly contributed to the elucidation of strongly correlated electron systems, as well as their unconventional superconductivity. Theoretical and experimental research of superconductivity of κ-$(ET)_2X$ [ET: bis(ethylenedithio)tetrathiafulvalene, X: monovalent anion], high-T_c cuprates and some heavy-fermion systems suggests that its emergence may involve antiferromagnetic (AF) spin fluctuation [1–4]. Since the AF spin interactions are likely to contribute to the emergence of superconductivity, the relationship between superconductivity and the magnetic properties could reveal the pairing mechanism behind unconventional superconductors.

Among the organic conductors, a quasi-two dimensional charge transfer salt λ-$(BETS)_2GaCl_4$ [BETS: bis(ethylenedithio)tetraselenafulvalene] has been actively researched because it shows interesting phenomena. λ-$(BETS)_2GaCl_4$ is a paramagnetic metal that exhibits a superconducting (SC) transition at 6 K at ambient pressure [5]. It has attracted much attention because a d-wave SC gap structure has been reported in a thermodynamic study [6]. In addition, the possibility of the Fulde-Ferrell-Larkin-Ovchinnikov state near the upper critical field has been suggested by several experiments [7–9].

Figure 1(b) shows the pressure–temperature (P-T) phase diagram of λ-$(D)_2GaCl_4$, where D = ET, us-STF or BETS and whose molecular structures are shown in Fig. 1(a) [10–12]. The us-STF denotes unsymmetrical-bis(ethylenedithio)diselenadithiafulvalene. The donor molecules, D, differ by their chalcogen atoms, i.e., sulfur or selenium atoms. Changing the inner chalcogen atoms from sulfur to selenium efficiently increases the transfer integrals, inducing an itinerancy in their electronic system. Hence, in the P-T phase diagram, λ-$(BETS)_2GaCl_4$ is located in the higher pressure region, whereas λ-$(ET)_2GaCl_4$ is in the low-pressure region.

The phase diagram of λ-$(BETS)_2GaCl_4$ has also been investigated in the alloy system λ-$(BETS)_2GaBr_xCl_{4-x}$ ($0 \leqslant x \leqslant 2$) [Fig. 1(c)] [10]. As x increases, the cell volume increases, thereby decreasing the effective transfer integrals. As a result, the insulating phase is induced where x is large. Resistivity measurements revealed that when $x = 0.75$, an metal-insulator transition occurs around 13 K [14]. Recent ^{13}C NMR studies revealed the existence of a commensurate spin density wave– (SDW) ordered phase below 13 K [13], indicating that an SDW ordered phase adjacent to the SC phase in λ-$(BETS)_2GaCl_4$. Actually, ^{13}C NMR measurements for λ-$(BETS)_2GaCl_4$ at ambient pressure revealed that, below 10 K, the spin-lattice relaxation rate divided by temperature $(1/T_1T)$ increased with decreasing temperature, indicating the existence of SDW fluctuation even in the sample with $x = 0.0$ [15].

Considering the above, the relationship between SDW fluctuation and the superconductivity in λ-$(BETS)_2GaCl_4$ should be investigated. Incidentally, an SDW phase is adjacent to the SC phase in the well-known organic conductor $(TMTSF)_2PF_6$ [16]. ^{13}C NMR measurements of $(TMTSF)_2PF_6$ under pressure have revealed that $1/T_1T$ is significantly increased at low temperatures, indicating the development of SDW fluctuation [17]. In addition, the pressure dependence of the SDW fluctuation correlates well with that of the superconducting transition temperature (T_c), implying an essential connection between SDW fluctuation and the emergence of superconductivity.

*m_sawada@eis.hokudai.ac.jp
†atkawa@phys.hokudai.ac.jp

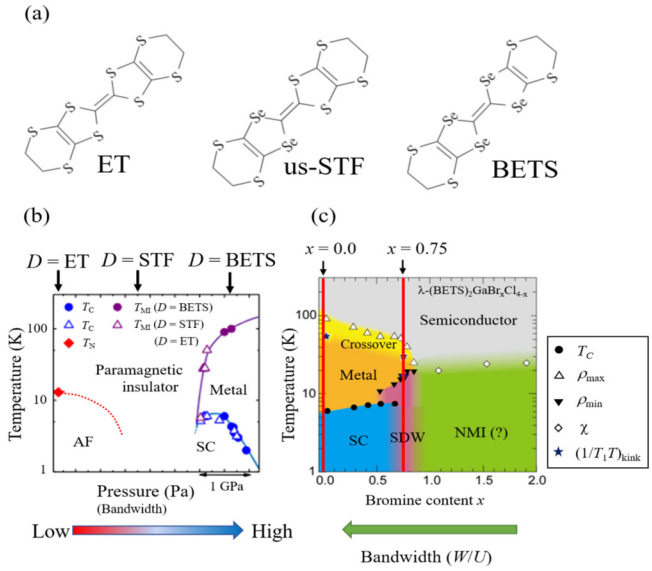

FIG. 1. (a) Molecular structures of the ET, us-STF, and BETS. (b) The P-T phase diagram of λ-$(D)_2GaCl_4$ for the three compounds, D = ET, us-STF, or BETS [10–12]. (c) The phase diagram of λ-$(BETS)_2GaBr_xCl_{4-x}$ with x ranging from 0 to 2 [10,13]. The left side of this diagram is akin to a high pressure (large U/W) region.

Contrary, in κ-type organic conductors,the SC phase is adjacent to an AF insulating phase [18]. ^{13}C NMR measurement of κ-$(ET)_2Cu(NCS)_2$ under pressure has revealed that the Korringa factor is larger than unity, suggesting the existence of AF spin correlations and that the pressure dependence of the Korringa factor correlates well with T_c [19]. Therefore, in λ-$(BETS)_2GaCl_4$, it is worthwhile to investigate which of the spin fluctuation effects, such as SDW fluctuation and the Korringa factor, are correlated with the superconductivity.

In λ-$(BETS)_2GaCl_4$, the SDW fluctuation has only been investigated at ambient pressure. Hence, it is desirable to investigate the pressure dependence of SDW fluctuation in λ-$(BETS)_2GaCl_4$ to elucidate the relationship between SDW fluctuation and superconductivity. In a previous study, T_c was suppressed when pressure was applied, and the electronic system became FL state above a critical pressure [10]. Hence the pressure dependence of the Korringa factor is also informative. We report the results of ^{13}C NMR measurements of λ-$(BETS)_2GaCl_4$ under pressure, focusing on the pressure effect on SDW fluctuations and Korringa factor qualitatively.

II. EXPERIMENTS

Single crystals of λ-$(BETS)_2GaCl_4$ were synthesized by the standard electrochemical method [20]. The crystal structure is shown in Fig. 2(a) and the isotope labeled molecular structure of BETS is shown in Fig. 2(b). Note that one ^{13}C was incorporated into the central double bond to avoid Pake doublets [Fig. 2(b)] [21]. The carbon site on central double bond is suitable for ^{13}C NMR measurements because the electron density of the highest occupied molecular orbital (HOMO) is sufficiently high, enabling the ^{13}C NMR to be carried out with a good sensitivity. The typical size of the sample used in the NMR measurements is $3.0\times0.5\times0.1$ mm^3. A NiCrAl cramp

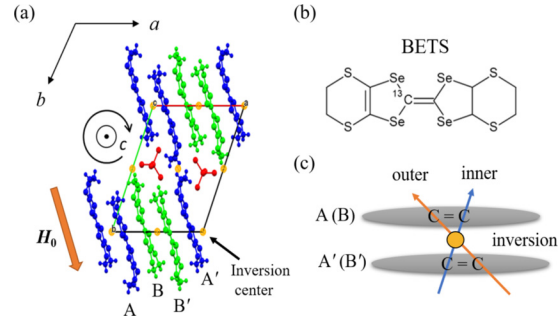

FIG. 2. (a) The crystal structure of λ-$(BETS)_2GaCl_4$. The applied magnetic field direction is parallel to the long axis of BETS molecule. (b) The BETS molecule was enriched with ^{13}C at the central double bond. (c) The schematic of inequivalent ^{13}C sites.

cell and Daphne 7474 oil as a pressure medium were used. The applied pressures, 3, 6, and 11 kbar, were calibrated at low temperature. The NMR measurements were done on the samples in a 6.0 T magnetic field in the direction in which the hyperfine coupling constant was the smallest, that is, almost parallel to the long axis of BETS molecule [see Fig. 2(a)]. This direction is convenient because the spin-lattice relaxation time (T_1) is at its smallest and almost all the peaks are superposed [15]. To obtain separated peaks, we set the magnetic field slightly tilted from the molecular long axis. In this field direction, the upper critical field at 1.5 K is substantially lower than 6 T, so the SC sate is completely suppressed. The NMR spectra were obtained by fast Fourier transformation of the echo signal with $\pi/2$-π pulse sequences. The typical value with $\pi/2$ pulse length was 1.5 μs. The NMR shifts were referenced to that of tetramethylsilane (TMS). T_1 was measured by the conventional saturation-recovery method.

III. RESULTS

A. NMR shift at ambient pressure

As shown in Fig. 2(a), λ-$(BETS)_2GaCl_4$ salt has two crystallographically inequivalent molecules A and B, which have equivalent molecules linked by inversion symmetry A′ and B′, respectively [see Fig. 2(a)]. In addition, there are two crystallographically inequivalent ^{13}C sites ("inner" and "outer" sites) [see Fig. 2(c)], so that four peaks can be expected in NMR spectra. The deviation of the resonance frequency from the standard sample (TMS) is called an NMR shift (δ), and it contains various information. In general, the NMR shift is expressed as the sum of the Knight shift (K_s) and the chemical shift (σ); $\delta = K_s + \sigma$. The Knight shift is proportional to the local spin susceptibility of the electrons (χ_s), that is, $K_s = A_{hf}\chi_s$, where, A_{hf} is a hyperfine coupling constant. We can evaluate χ_s from K_s and A_{hf}. Note that σ is unique for a molecule and is usually temperature independent. In addition to these, the magnetism of the pressure cell (χ_{cell}) should also be taken into account, so the NMR shift can be written as $\delta = A_{hf}\chi_s + \sigma + B\chi_{cell}$, where B is a constant. Although we need to estimate $B\chi_{cell}$ and σ experimentally to evaluate χ_s, fortunately, we observed that the four peaks were slightly separated because of the slightly off-axial field direction. Hence, we used the difference in the NMR shifts to cancel

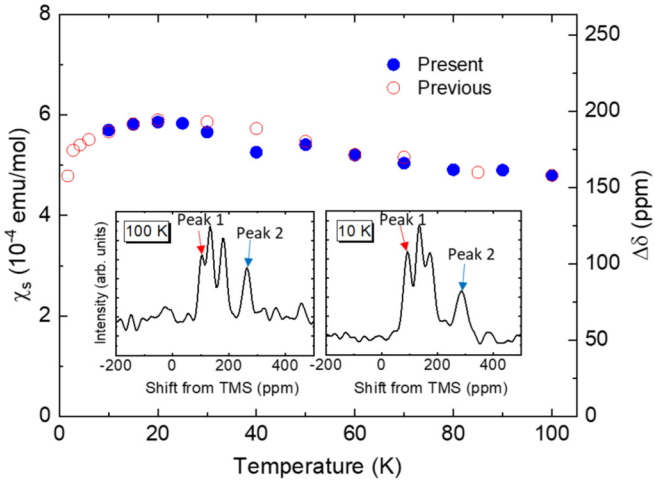

FIG. 3. Temperature dependence of the local spin susceptibility (left axis) and the difference in NMR shift $\Delta\delta$ (right axis) at ambient pressure. The blue and red circles indicate the results of the present study and a previous study, respectively [15]. The inset shows the NMR spectra at 100 K and 10 K at ambient pressure. The red and blue arrows indicate Peak 1 and Peak 2, respectively.

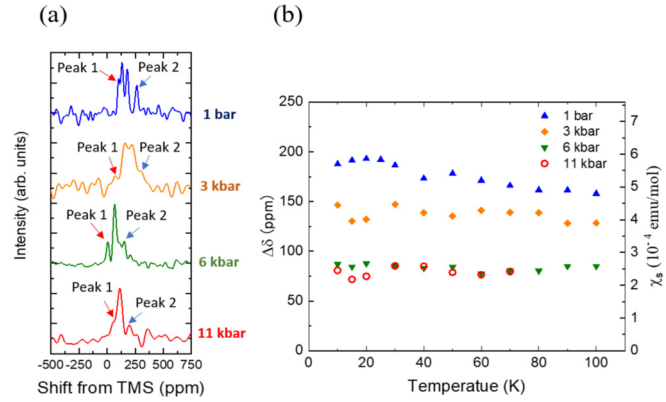

FIG. 4. (a) NMR spectra under each pressure at 50 K. The red and blue arrows instruct the Peak 1 and Peak 2, respectively. (b) The temperature dependence of local spin susceptibility (left) and the difference of NMR shift (right) under pressure.

out the effect of $B\chi_{\rm cell}$ and σ. Note that $B\chi_{\rm cell}$ and σ can be regarded as having the same values for all four peaks [22]. We assigned the distant peaks in the spectrum as Peak 1 and Peak 2, respectively (see the inset of Fig. 3). The NMR shifts for these two peaks can be expressed as the following Eq. (1) and Eq. (2), and their difference as Eq. (3),

$$\delta_1 = A_{\rm hf1}\chi_s + \sigma + B\chi_{\rm cell}, \tag{1}$$

$$\delta_2 = A_{\rm hf2}\chi_s + \sigma + B\chi_{\rm cell}, \tag{2}$$

$$\Delta\delta = \delta_2 - \delta_1 = (A_{\rm hf2} - A_{\rm hf1})\chi_s. \tag{3}$$

The right axis in Fig. 3 represents the temperature dependence of $\Delta\delta$ at ambient pressure which is obtained from the difference in the NMR shifts of Peaks 1 and 2. The coefficient $A_{\rm hf2} - A_{\rm hf1}$ ($\approx$1.9 kOe/μ_B) was determined such that the value of the local spin susceptibility at 100 K was completely consistent with that of a previous ^{13}C NMR study [15]. This enabled us to obtain the temperature dependence of χ_s, since the coefficient $A_{\rm hf2} - A_{\rm hf1}$ is temperature independent. As shown in Fig. 3, our results replicate those of the previous study well for the whole temperature range. Moreover, χ_s shows a broad humped structure near 20 K, as in the previous study [15]. The similarities with the previous study is strong support for the validity of our analysis.

B. NMR shift under pressure

The temperature dependence of χ_s under pressure was also evaluated in the same manner. Figure 4(a) shows the NMR spectra taken at ambient pressure and at pressures of 3, 6 and 11 kbar at 50 K. The spectrum at 3 kbar looks broader, which is thought to be due to the strain associated with the pressure. At 11 kbar, signals from the Daphne oil appeared in the spectrum at around 80–100 K because T_1 of λ-$(BETS)_2GaCl_4$ was relatively longer, and this made it difficult to assign Peaks 1 and 2. Below 70 K, the signal from the oil could be removed because the T_1 of the sample became sufficiently shorter than that of the oil. Therefore, when the pressure was 11 kbar, we used only data obtained when the temperature was below 70 K. The broad hump structure around 20 K observed at ambient pressure is suppressed by applying pressure, and χ_s exhibits almost temperature-independent behavior at 6 and 11 kbar. This indicates that the electronic system exhibits a Fermi liquid state over a wider temperature range under pressure. Moreover, the absolute value of χ_s is reduced under pressure. This can be attributed to the reduction of the density of states (DOS) at the Fermi surface since the bandwidth is widened by applying pressure.

C. Spin-lattice relaxation time T_1

The spin-lattice relaxation time T_1 provides significant information on spin fluctuations. In our measurements, T_1 was evaluated from the peaks comprising four ^{13}C sites. Since each ^{13}C site has a slightly different T_1, the recovery profiles deviate from the single exponential function. To correct this deviation, we used a stretched exponential function, $M(t) = M_0\{1 - \exp(-t/T_1)^\beta\}$. Here $M(t)$ and M_0 are the nuclear magnetizations at time t and at thermal equilibrium, respectively, and β is the stretching exponent. In a previous report, β was set as 0.8 for the whole temperature range [15]. To ensure that the recovery profile does not change under pressure, we plotted $\log\{[M_0 - M(t/T_1)]/M_0\}$ against t/T_1, as shown in Fig. 5. The solid curve shows the stretched exponential function with $\beta = 0.8$. The experimental data agree with the solid curve even under pressure, indicating that the recovery profile does not change.

Figure 6 shows the temperature dependence of $1/T_1T$. Our results at ambient pressure are consistent with those obtained in a previous study at ambient pressure, shown in the inset [15]. At ambient pressure, $1/T_1T$ increases as the temperature is lowered and peaks at 55 K, which is denoted by T^*. T^* can be seen at 70 K when the pressure was 3 kbar. At 6 and 11 kbar, it is difficult to determine T^* because T^* is thought to have shifted to above 100 K. At 11 kbar, $1/T_1T$ becomes almost constant in the whole temperature range.

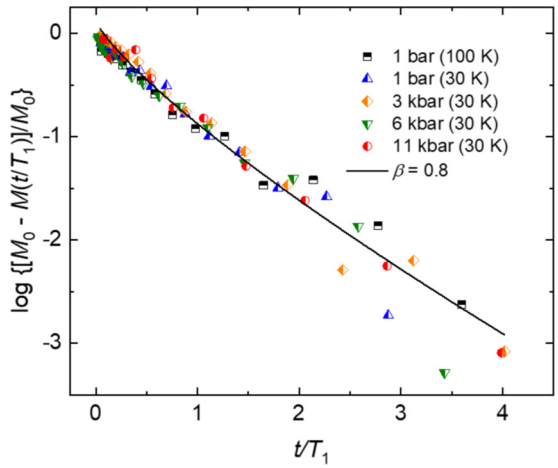

FIG. 5. The plot of recovery curves at ambient (100 and 30 K) and under each pressure at 30 K. The solid line is the fitting plot with $\beta = 0.8$.

IV. DISCUSSION

A. $1/T_1T$ above T^*

In this section, we discuss the behavior of $1/T_1T$ above T^*. Generally, $1/T_1T$ is written as,

$$\frac{1}{T_1T} = \frac{2\gamma_n^2 k_B}{(\gamma_e\hbar)^2}\sum_q A_\perp^2(q)\frac{\chi_\perp''(q)}{\omega}, \tag{4}$$

where, γ_n and γ_e are the gyromagnetic ratios of nuclear and electron spins, respectively, k_B is the Boltzmann constant, and $\hbar$ is the reduced Planck constant. $A_\perp(q)$ and $\chi_\perp''(q)$ represent the hyperfine coupling constant and the imaginary part of the dynamic spin suceptibility perpendicular to the field direction with wave vector q, respectively [23]. ω is an angular frequency in NMR measurements. When the system has a two-dimensional AF spin fluctuation, the temperature dependence of $1/T_1T$ can be described by the Curie-Weiss function,

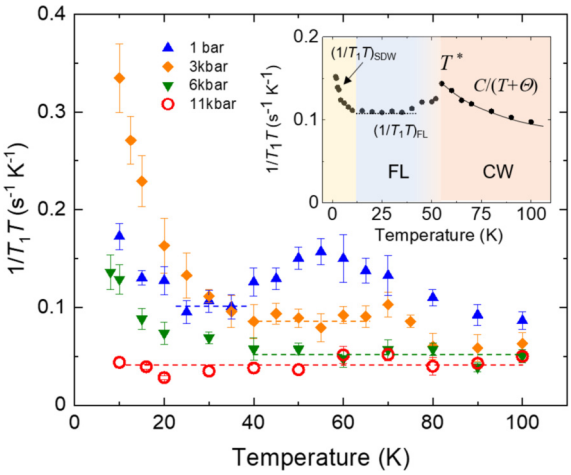

FIG. 6. Temperature dependence of $1/T_1T$ at ambient and at pressures of 1, 3, 6, and 11 kbar. The inset shows the results of a previous study at ambient pressure [15]. The dashed lines are a visual aid for the averaged values in the FL state.

$1/T_1T = C/(T+\Theta)$, as shown in the inset of Fig. 6 [24]. Here, C and Θ correspond to the Curie constant and Weiss temperature, respectively. In a previous study, it has been suggested that the increase in $1/T_1T$ at high temperatures can be attributed to the AF spin fluctuation derived from the localized electron system, as confirmed in the dimer Mott system of λ-$(ET)_2GaCl_4$ [15]. Our results show that T^* shifts to a higher temperature region when pressure is applied. T^* has also been reported to behave similarly in κ-$(ET)_2Cu(NCS)_2$ [19]. Since the metal-semiconductor crossover occurs at T^*, these results indicate increased itinerancy when pressure is applied. This is also supported by the reduction of DOS with the widening of bandwidth.

B. $1/T_1T$ below T^*

In this section, we focus on the behavior of $1/T_1T$ below T^*. At ambient pressure, $1/T_1T$ shows temperature-independent behavior below T^* down to 10 K, indicating a FL state. Below 10 K, $1/T_1T$ increases as temperature decreases. This increase in $1/T_1T$ can be attributed to the SDW fluctuation, since the SDW ordered phase has been confirmed in λ-$(BETS)_2GaBr_{0.75}Cl_{3.25}$. Therefore, $1/T_1T$ below T^* can be described by the sum of two terms, one originating from SDW fluctuations $(1/T_1T)_{SDW}$ and the other from the itinerant electron system $(1/T_1T)_{FL}$, as follows:

$$\frac{1}{T_1T} = \left(\frac{1}{T_1T}\right)_{SDW} + \left(\frac{1}{T_1T}\right)_{FL}. \tag{5}$$

Here $(1/T_1T)_{FL}$ was determined by the averaged value of $1/T_1T$ in the FL state, indicated by the dotted lines in Fig. 6. This term will be discussed in Sec. IV C. Regarding the term $(1/T_1T)_{SDW}$, the increase in $1/T_1T$ at 3 kbar is greater than that at ambient pressure, indicating that the SDW fluctuation is enhanced by applying pressure. At 6 kbar, the increase in $1/T_1T$ still remains at low temperatures, although the degree of increase in $1/T_1T$ is less than that at 3 kbar. At 11 kbar, the increase in $1/T_1T$ is mostly suppressed, indicating disappearance of the SDW fluctuation. The temperature-independent behavior of $1/T_1T$ at 11 kbar indicates that the electron system becomes Fermi liquid down to the lowest temperature.

C. Korringa factor

Next, we focus on $(1/T_1T)_{FL}$, which reflects the DOS at the Fermi energy $[N(E_F)]$ and provides important information about electron correlation. Since the electronic state is itinerant, $(1/T_1T)_{FL}$ satisfies the Korringa relation as follows:

$$\frac{1}{(T_1T)_{FL}K_s^2} = \left(\frac{A_\perp}{\sqrt{2}A_\parallel}\right)^2\frac{4\pi k_B}{\hbar}\left(\frac{\gamma_n}{\gamma_e}\right)^2\mathcal{K}, \tag{6}$$

where, $\mathcal{K}$ is the Korringa factor. Usually, the Korringa factor characterizes the electron correlation, with a value of 1 expected for electronic systems of normal metals, and a values of >1 and <1 for electronic systems with antiferromagnetic and ferromagnetic correlations, respectively. In order to evaluate the form factor $(A_\perp/\sqrt{2}A_\parallel)$, we utilized the hyperfine coupling tensor of κ-$(ET)_2Cu(NCS)_2$ which has a similar dimer structure. Although BETS is the Se analog of the ET molecule, the HOMO electron density at the ^{13}C in BETS is

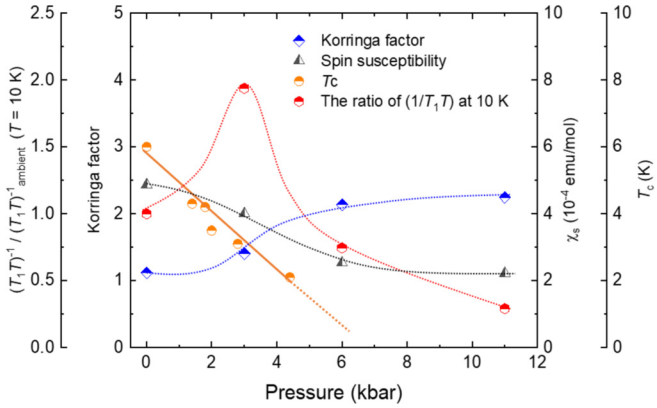

FIG. 7. Pressure dependence of Korringa factor, spin susceptibility, the ratio of $1/T_1T$ at 10 K which is divided by the value at ambient pressure, and superconducting T_C [10]. The dashed lines are a visual aid. The ratio of $1/T_1T$ at 10 K corresponds to the strength of the SDW fluctuation.

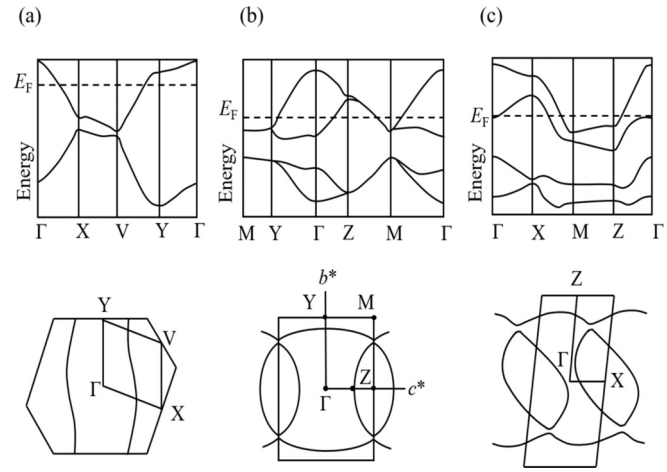

FIG. 8. The schematics of Fermi surface for (a) $(TMTSF)_2PF_6$, (b) κ-$(ET)_2Cu(NCS)_2$, and (c) λ-$(BETS)_2GaCl_4$ [27–29].

similar to that in ET. In addition, the overlap mode of a dimer, the "ring–over–bond," are the same for both κ type and λ type [10,25]. Therefore, the form factor $(A_\perp/\sqrt{2}A_\parallel)$ can be roughly evaluated from the hyperfine coupling tensor $\mathbf{A}$ as follows:

$$\mathbf{A} = \begin{pmatrix} a_{xx} & a_{xy} & a_{xz} \\ a_{yx} & a_{yy} & a_{yz} \\ a_{zx} & a_{zy} & a_{zz} \end{pmatrix}, \tag{7}$$

$$\left(\frac{A_\perp}{\sqrt{2}A_\parallel}\right)^2 = \frac{a_{xx}^2 + a_{yy}^2 + 2a_{xy}^2 + a_{zx}^2 + a_{zy}^2}{2a_{zz}^2}, \tag{8}$$

where the z axis is set parallel to the molecular long axis. We used the mean value of the hyperfine coupling tensor of the inner and outer ^{13}C sites of κ-$(ET)_2Cu(NCS)_2$ [25]. The Korringa factor values were evaluated using Eqs. (6) and (8), and are given in Fig. 7 with the spin susceptibility, the $1/T_1T$ at 10 K and Tc. Although the local spin susceptibility decreases with increasing pressure, the Korringa factor increases with increasing pressure. At 3 kbar, it increases gradually, while at 6 and 11 kbar, it becomes approximately double compared to its value at ambient pressure, indicating that a significant change in electron correlation occurs above 6 kbar.

D. Comparison with other organic conductors

In κ-$(ET)_2Cu(NCS)_2$, the Korringa factor is much greater than unity ($\mathcal{K} \approx 8$) [19], indicating strong AF spin correlation, and it decreases with increasing pressure. Moreover, the Korringa factor and T_c correlate with each other, implying that the AF spin correlation plays a crucial role in the emergence of superconductivity in κ-type salts [19]. In $(TMTSF)_2PF_6$, the Korringa factor is almost constant even under pressures, and is close to unity, indicating weak electron correlation [17]. In addition, the strength of SDW fluctuation correlates well with T_c, since SDW fluctuation is probably essential for the emergence of superconductivity in $(TMTSF)_2PF_6$. In λ-$(BETS)_2GaCl_4$, the Korringa factor is close to unity below 3 kbar, indicating weak electron correlation in contrast to κ-$(ET)_2Cu(NCS)_2$. Remarkably, the Korringa factor at 6 and 11 kbar becomes roughly double compared to its value at ambient pressure, indicating a significant change in electron correlation. Moreover, the SC phase appears in the weakly correlated electronic state with SDW fluctuations. On the other hand, the strength of the SDW fluctuations is not correlated with T_c, unlike in $(TMTSF)_2PF_6$. From theory, it has been suggested that magnetic fluctuation can contribute to not only to the formation of Cooper pairs but also to their destruction [26]. Usually, T_c also depends on DOS at the Fermi energy. The DOS, which was estimated from the local spin susceptibility, is reduced by about 50% under pressure in λ-$(BETS)_2GaCl_4$. This reduction is greater than that for κ-$(ET)_2Cu(NCS)_2$ [19], suggesting the suppression of T_c under pressure in λ-$(BETS)_2GaCl_4$ is mainly governed by the reduction of DOS at the Fermi energy.

These differences may originate from a difference in dimensionality and the shape of the Fermi surface. Figure 8 shows the schematic of the Fermi surface for (a) $(TMTSF)_2PF_6$, (b) κ-$(ET)_2Cu(NCS)_2$, and (c) λ-$(BETS)_2GaCl_4$. $(TMTSF)_2PF_6$ and κ-$(ET)_2Cu(NCS)_2$ have simple a quasi-one-dimensional (quasi-1D) and a two-dimensional (2D) Fermi surface, respectively [28,29]. On the other hand, λ-$(BETS)_2GaCl_4$ has multi-band Fermi surfaces with quasi-1D and 2D [27,30]. In a single-band system, the effect of applying pressure mainly causes the widening of bandwidth, but it can also change the shape of the Fermi surface. This deformation of the Fermi surface may occur under pressure in λ-$(BETS)_2GaCl_4$, and significantly change the electron correlation. From this point of view, the pressure dependence of superconducting T_c seems to be related to the change in electron correlation, that is, the almost complete disappearance of T_c accompanied by suppression of the SDW fluctuations in the region where the electron correlation changed. Further practical and theoretical studies are warranted to investigate in detail the relationship between T_c and SDW fluctuation.

The anomalous enhancement of $1/T_1T$ at a pressure of 3 kbar can also be explained by deformation of the Fermi surface. First, the nesting condition becomes suitable for SDW fluctuation at 3 kbar, and then, deformation of the Fermi surface may disturb the nesting condition, resulting in

the disappearance of the SDW fluctuations under pressure. Measuring the angular dependence of magnetoresistance oscillations may shed light on the Fermi surface change under pressure.

Alternative possibilities should also be considered. In $(TMTSF)_2PF_6$ and the pnictide superconductor $Ba(Fe_{1-x}Co_x)_2As_2$, the temperature dependence of electric resistivity shows T-linear behavior at low temperature just above the SC phase [31]. This behavior is a typical characteristic of a non-Fermi liquid state, and theoretical studies suggest that the non-Fermi liquid state appears near a quantum critical point [32]. Since this fluctuation might not be a thermal one, it might be the origin of the enhancement of $1/T_1T$ at 3 kbar.

V. CONCLUSION

We performed ^{13}C NMR measurements of a single crystal of λ-$(BETS)_2GaCl_4$ under pressure. We found that the local spin susceptibility decreases under pressure, corresponding to a reduction in DOS at the Fermi energy. The behavior of $1/T_1T$ in the high temperature region and T^* is similar in both λ-$(BETS)_2GaCl_4$ and κ-$(ET)_2Cu(NCS)_2$, but the strengths of their electron correlation are different. We have also confirmed an increase in $1/T_1T$ in the low-temperature region, which can be attributed to SDW fluctuation. Unlike in $(TMTSF)_2PF_6$, the increase in $1/T_1T$ is significantly enhanced when 3 kbar is applied, indicating enhancement of the SDW fluctuation. In contrast, the $1/T_1T$ increase at low temperatures is reduced at 6 kbar and is completely suppressed at 11 kbar. Moreover, the Korringa factor is increased above 6 kbar, indicating a significant change in electron correlation. This behavior differs from that of κ-$(ET)_2Cu(NCS)_2$ and $(TMTSF)_2PF_6$, and this can be attributed to the multiband system of the Fermi surface. The suppression of SDW fluctuation is likely to be related to the change in the electron correlation under pressure. We revealed that the superconductivity appears in the weakly correlated electronic state with SDW fluctuations. There is still no consensus how the SDW fluctuation contributes to superconductivity, so further practical and theoretical research is required.

ACKNOWLEDGMENTS

The authors thank N. Matsunaga for setting up the high pressure cell. This study was partly supported by Hokkaido University, Global Facility Center (GFC), Advanced Physical Property Open Unit (APPOU), funded by MEXT under "Support Program for Implementation of New Equipment Sharing System" (JPMXS0420100318).

[1] H. Kondo and T. Moriya, J. Phys. Soc. Jpn. **67**, 3695 (1998).
[2] J. Schmalian, Phys. Rev. Lett. **81**, 4232 (1998).
[3] K. H. Bennemann and J. B. Ketterson (eds.), *Superconductivity* (Springer, Berlin, 2008).
[4] R. H. McKenzie, Science **278**, 820 (1997).
[5] H. Kobayashi, H. Tomita, T. Udagawa, T. Naito, and A. Kobayashi, Synth. Met. **70**, 867 (1995).
[6] S. Imajo, S. Yamashita, H. Akutsu, H. Kumagai, T. Kobayashi, A. Kawamoto, and Y. Nakazawa, J. Phys. Soc. Jpn. **88**, 023702 (2019).
[7] M. A. Tanatar, T. Ishiguro, S. Kagoshima, N. D. Kushch, and E. B. Yagubskii, Phys. Rev. B **65**, 064516 (2002).
[8] W. A. Coniglio, L. E. Winter, K. Cho, C. C. Agosta, B. Fravel, and L. K. Montgomery, Phys. Rev. B **83**, 224507 (2011).
[9] S. Uji, K. Kodama, K. Sugii, T. Terashima, T. Yamaguchi, N. Kurita, S. Tsuchiya, T. Konoike, M. Kimata, A. Kobayashi, B. Zhou, and H. Kobayashi, J. Phys. Soc. Jpn. **84**, 104709 (2015).
[10] H. Tanaka, A. Kobayashi, A. Sato, H. Akutsu, and H. Kobayashi, J. Am. Chem. Soc. **121**, 760 (1999).
[11] T. Minamidate, Y. Oka, H. Shindo, T. Yamazaki, N. Matsunaga, K. Nomura, and A. Kawamoto, J. Phys. Soc. Jpn. **84**, 063704 (2015).
[12] H. Mori, M. Kamiya, H. Suzuki, M. Suto, S. Tanaka, Y. Nishio, K. Kajita, and H. Moriyama, J. Phys. Chem. Solids **63**, 1239 (2002).
[13] T. Kobayashi, T. Ishikawa, A. Ohnuma, M. Sawada, N. Matsunaga, H. Uehara, and A. Kawamoto, Phys. Rev. Research **2**, 023075 (2020).
[14] H. Tanaka, T. Adachi, E. Ojima, H. Fujiwara, K. Kato, H. Kobayashi, A. Kobayashi, and P. Cassoux, J. Am. Chem. Soc. **121**, 11243 (1999).
[15] T. Kobayashi and A. Kawamoto, Phys. Rev. B **96**, 125115 (2017).
[16] D. Jérome, Science **252**, 1509 (1991).
[17] Y. Kimura, M. Misawa, and A. Kawamoto, Phys. Rev. B **84**, 045123 (2011).
[18] K. Kanoda, Hyperfine Interact. **104**, 235 (1997).
[19] M. Itaya, Y. Eto, A. Kawamoto, and H. Taniguchi, Phys. Rev. Lett. **102**, 227003 (2009).
[20] H. Kobayashi, T. Udagawa, H. Tomita, K. Bun, T. Naito, and A. Kobayashi, Chem. Lett. **22**, 1559 (1993).
[21] G. E. Pake, J. Chem. Phys. **16**, 327 (1948).
[22] T. Kawai and A. Kawamoto, J. Phys. Soc. Jpn. **78**, 074711 (2009).
[23] T. Moriya, J. Phys. Soc. Jpn. **18**, 516 (1963).
[24] T. Moriya and K. Ueda, Rep. Prog. Phys. **66**, 1299 (2003).
[25] Y. Saito and A. Kawamoto, Solid State Nucl. Magn. Reson. **73**, 22 (2016).
[26] S. S. Saxena, K. Ahilan, T. E. Weller, M. Ellerby, R. P. Smith, N. T. Skipper, S. Rowley, A. Kusmartseva, and G. G. Lonzarich, Iran. J. Phys. Res. **6**, 129 (2006).
[27] L. Montgomery, T. Burgin, J. Huffman, J. Ren, and M.-H. Whangbo, Physica C **219**, 490 (1994).
[28] K. Oshima, T. Mori, H. Inokuchi, H. Urayama, H. Yamochi, and G. Saito, Phys. Rev. B **38**, 938 (1988).
[29] P. M. Grant, J. Phys. Paris **C3-847**, 938 (1988).
[30] C. Mielke, J. Singleton, M.-S. Nam, N. Harrison, C. C. Agosta, B. Fravel, and L. K. Montgomery, J. Phys.: Condens. Matter **13**, 8325 (2001).
[31] N. Doiron-Leyraud, P. Auban-Senzier, S. René de Cotret, C. Bourbonnais, D. Jérome, K. Bechgaard, and L. Taillefer, Phys. Rev. B **80**, 214531 (2009).
[32] H. v. Löhneysen, A. Rosch, M. Vojta, and P. Wölfle, Rev. Mod. Phys. **79**, 1015 (2007).